Wave simulation using SWAN in nested and unnested mode applications

Roop Lalbeharry[1] and Hal Ritchie[2]
Environment Canada

[1]Meteorological Research Division, Toronto, ON M3H 5T4
[2]Meteorological Research Division, Dartmouth, NS B2Y 2N6

1. Introduction

The development of wave forecasting models which can predict sea states in a consistent way for all marine activities is a challenging task. Not only do nearshore marine activities require different information on different spatial and time scales than (for example) shipping activities, but also the physical processes which affect wave growth, propagation and decay differ considerably in nearshore areas compared to open ocean areas. The European community model WAM, widely used in operational wave forecasting, was originally developed for deep water only, and is typically applied at relatively low horizontal resolution, with grid lengths greater than 20 km (WAMDI Group, 1988). Later, the model SWAN (Simulation of Waves Nearshore) was developed, using WAM as a basis, but designed for application in coastal waters (Holthuijsen, 2007; Booij et al., 1999; Ris et al., 1999). This model has been applied at the higher spatial resolution needed for more accurate simulation of the effects of complex shorelines and bottom topography. Earlier investigations with WAM Cycle-4.0 (hereafter referred as WAM4) applied to coastal seas or lakes (e.g. Monbaliu et al., 2000; Liu et al., 2002; Soomere et al., 2005) demonstrated that such an open ocean model can perform practically as well as specific coastal wave models (such as the SWAN model described in Section 2) in terms of the basic wave parameters since this model follows the principles of WAM. Some of the high resolution small-scale enhancements of WAM4 introduced by Monbaliu et al. (2000) have been included in later versions of WAM such as WAM Cycle-4.5 (hereafter referred as WAM4.5) used in this study.

SWAN Cycle-III version 40.31, and subsequently the most recent version 40.72 are applied in both nested and unnested modes to simulate waves associated with an extreme storm event in the northwest Atlantic and over Lake Erie at different grid resolutions. The wave growth limiter of Hersbach and Janssen (1999) is added as an option and is used when the WAM4 option is chosen in SWAN. In the original implementation of the SWAN version of WAM4, the shift growth parameter was omitted in the wind input source term. The omission of this parameter apparently led to underprediction of the significant wave heights. Inclusion of this parameter causes a slight enhancement of the normalized growth rate and results in better agreement with the observed wave heights. The three runs of SWAN include the run using the WAM Cycle-3 (hereafter referred as WAM3) described in WAMDI Group (1988) and based on Komen (1984)) physics, that using WAM4 based on Janssen (1989,1991) physics as originally implemented in SWAN and that using the modified implementation of SWAN WAM4 physics. For the northwest Atlantic storm WAM4.5 runs on a coarse grid while SWAN and a nested version of WAM4.5 run on a fine grid using the boundary conditions of the coarse grid WAM4.5. For Lake Erie both WAM4.5 and SWAN run on the same

grid using the same wind input. SWAN version 40.31 was originally applied to both cases (Lalbeharry et al., 2009a, 2009b) but in this study the two cases are revisited using the most recent SWAN 40.72 version as well as some results from version 40.31.

The general goal of the work reported in this paper is to evaluate the performances of WAM4.5 and SWAN in nested and unnested mode applications and to determine whether the coastal model SWAN is required to get reliable results or whether the ocean model WAM4.5 is capable enough to provide wave data of sufficient and acceptable accuracy and quality. Section 2 presents a brief description of the wave models used in this study while section 3 describes the model setup and wind input. Model results compared with buoy measurements are described in section 4 followed by conclusions in section 5.

2. The wave models WAM4.5 and SWAN

The two-dimensional wave action density spectrum $N(\sigma,\theta,\phi,\lambda,t)$ describes the ocean waves and is given as a function of relative angular frequency σ, wave direction θ (measured clockwise relative to true north), latitude ϕ, longitude λ, and time t. Here, $\sigma = [(gk)\tanh(kh)]^{1/2}$ in which k (= $2\pi/L$, L being the wavelength) is the wave number and is observed in a frame moving with the ocean current velocity, g is acceleration due to gravity and h is the water depth. The action density spectrum is defined as $N(\sigma,\theta,\phi,\lambda,t) = F(\sigma,\theta,\phi,\lambda,t)/\sigma$ in which $F(\sigma,\theta,\phi,\lambda,t)$ is the energy density spectrum. In general, the conservation equation for N in flux form in spherical coordinates and in frequency-direction space is governed by the transport equation given in the form:

$$\frac{\partial N}{\partial t} + (\cos\phi)^{-1}\frac{\partial}{\partial \varphi}(c_\varphi \cos\phi N) + \frac{\partial}{\partial \lambda}(c_\lambda N) + \frac{\partial}{\partial \sigma}(c_\sigma N) + \frac{\partial}{\partial \theta}(c_\theta N) = \frac{S}{\sigma} \qquad (1)$$

where

$$S = S_{phil} + S_{in} + S_{nl4} + S_{nl3} + S_{ds} + S_{bf} + S_{br} \qquad (2)$$

In Eq. (1) the first term on the left hand side represents the local rate of change of action density in time. The second and third terms represent the propagation of action density in geographical space (with propagation velocities c_ϕ and c_λ in latitude and longitude space, respectively). The fourth term gives the shifting of the relative frequency due to variations in depths and currents (with propagation velocity c_σ in σ space) and the fifth term the depth-induced and current-induced refraction (with propagation velocity c_θ in θ space). For zero current and time-independent depth $c_\sigma = 0$ and Eq. (1) reduces to the energy balance equation, that is, the 4th term on the left hand side vanishes and the depth refraction term (5th term) depends only on the depth gradient.

The term $S = S(\sigma,\theta,\phi,\lambda,t)$ on the right hand side of Eq. (1) is the net source term expressed in terms of energy density. It is the sum of a number of source terms given in Eq. (2) representing the effects of wave generation by wind (S_{phil} and S_{in}), quadruplet nonlinear wave-wave interactions (S_{nl4}), triad non-linear wave-wave interactions (S_{nl3}), dissipation due to whitecapping (S_{ds}), bottom friction (S_{bf}) and depth-induced wave breaking (S_{br}). The linear wind growth term S_{phil} is due to Cavaleri and Malonette-Rizzoli

(1981) but with a filter to eliminate contributions from frequencies lower than the Pierson-Moskowitz frequency (Tolman, 1992), and is hereafter referred as CR81. The exponential wind growth source term S_{in} is based on the formulations of Komen et al. (1984) in WAM3 and Janssen (1989, 1991) in WAM4. The source term S_{nl4} is the quadruplet nonlinear wave-wave interactions which transfers energy from spectral peaks to lower and higher frequencies. The energy is redistributed so that there is no net loss or gain of energy due to nonlinear wave-wave interactions. The S_{nl4} term dominates the evolution of the spectrum in deep and intermediate waters and is computed with the discrete interaction approximation method of Hasselmann et al. (1985). The bottom friction source term S_{bf} is based on the empirical Joint North Sea Wave Project (JONSWAP) model of Hasselmann et al. (1973) with the friction dissipation constant in S_{bf} being a tunable parameter set to 0.038 m^2s^{-3} in this study. The formulation of S_{br} is based on Battjes and Janssen (1978) while S_{nl3} is based on the lumped triad approximation of Eldeberky (1996). However, since WAM4.5 and SWAN are not applied in very shallow water or in the surf zone area in this study, the source terms S_{nl3} and S_{br} are generally small and are not activated in the models that contain one or both of them.

WAM solves the energy balance form of Eq. (1) for zero currents and fixed water depths on a spherical grid and in frequency-direction space. In WAM3 (WAMDI Group, 1988) S_{in} and S_{ds} in Eq. (2) are based on the formulations of Komen et al. (1984) while in WAM4 S_{in} and S_{ds} are based on the formulations of Janssen (1989, 1991) in which the winds and waves are coupled. WAM4.5 is an update of WAM4 and incorporates many of the changes described in Monbaliu et al. (2000). To ensure that WAM remains numerically stable a wave growth limiter based on the formulation of Hersbach and Janssen (1999) (hereafter referred as HJ99) is imposed, which gives the maximum total change of energy density per iteration per spectral wave component. More details of the formulation of WAM can be found in Komen et al. (1994).

SWAN solves the action balance equation on a spherical grid and in σ-θ space but because of the assumptions of time-independent water depths and no currents, the solution of Eq. (1) is equivalent to the solution of the energy balance equation as in WAM4.5. SWAN has the option of using WAM3 or WAM4 physics for the S_{in} and S_{ds} source terms with the default option being WAM3 and uses the wave growth limiter described in Ris (1997), hereafter referred as R97. The SWAN implementation of WAM4 is not consistent with the actual implementation of WAM4. The shift growth parameter $z_\alpha = 0.011$ in S_{in} is omitted and the limiter R97 instead of HJ99 is used. The modified S_{in} now includes z_α and a new subroutine is added so that when the WAM4 option is used, the limiter HJ99 is called. This correction is now added in all SWAN versions starting with version 40.51. The model results so produced are now in better agreement with those of WAM4.5 and WAM3. In this study SWAN Cycle-III version 40.72, the most recent version described in SWAN (2009), is used. Results based on SWAN version 40.31 described in SWAN (2004) are also presented to highlight the differences between the corrected and uncorrected implementations of SWAN WAM4. More details of SWAN are given in Booij et al. (1999) and Ris et al. (1999).

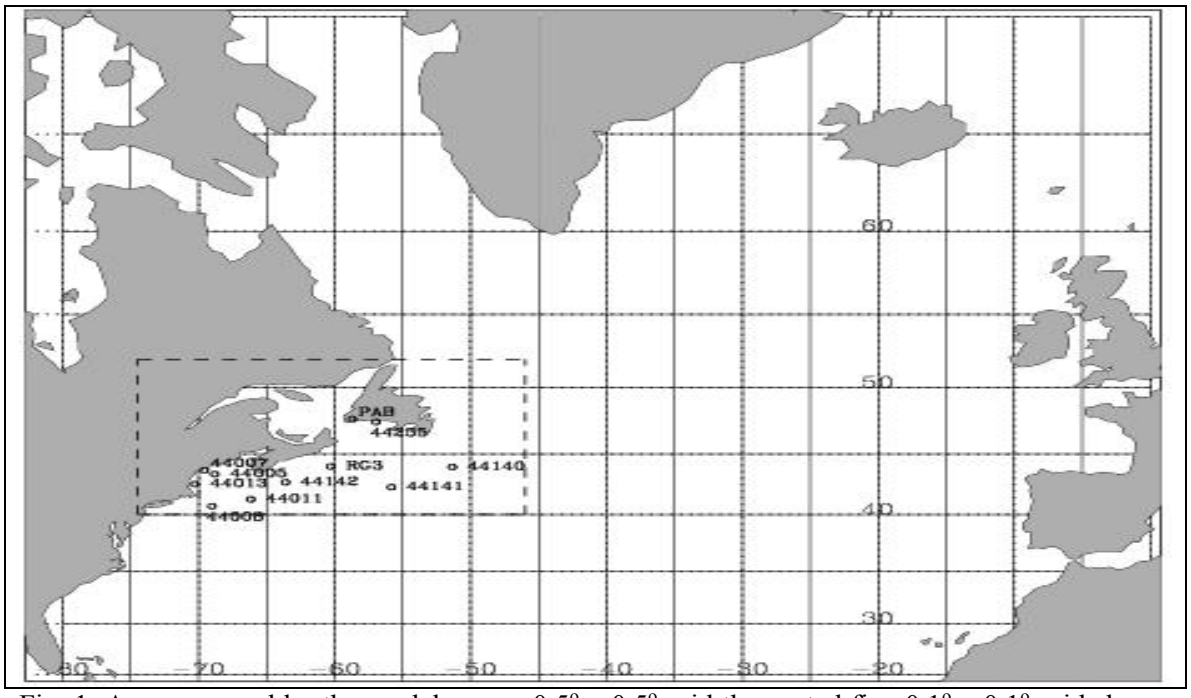

Fig. 1. Areas covered by the model coarse 0.5° x 0.5° grid the nested fine 0.1° x 0.1° grid shown as the enclosed box in broken lines. The locations of the buoys inside the fine grid area used for validation are also shown. RG3 is the drilling platform Rowan Gorilla III and PAB marks the location of Port-aux-Basques hit by two exceptionally large storm waves.

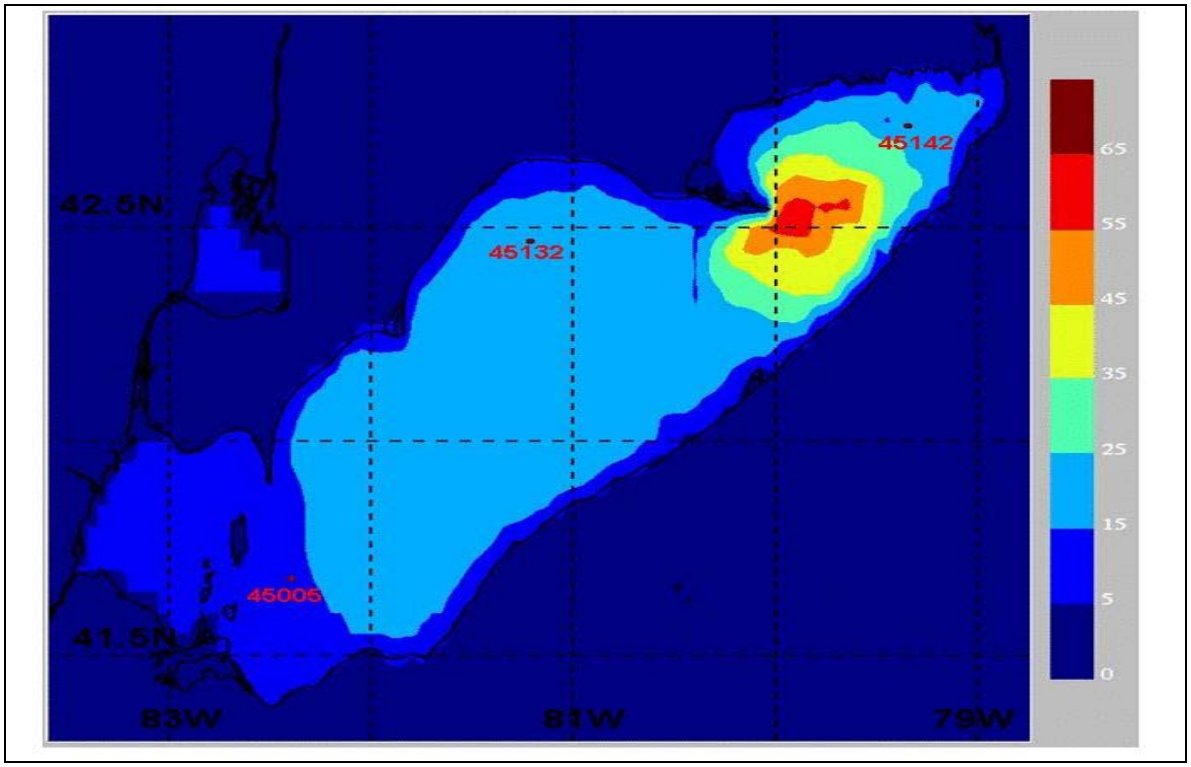

Fig. 2. Computational domain for Lake Erie. The figure also shows the bathymetry with water depths ranging from 5 to 60 m and the locations of buoys used in the verification of model results.

Table 1: WAM4.5 and SWAN options used in the January 2000 storm and Lake Erie case studies

Options	Physics	WAM4.5	SWAN		
			WAM 4	WAM4 +	WAM 3
S_{phil}	*Cavaleri and Malanotte-Rizzoli (1981); Tolman (1992)*	X	X	X	X
S_{in}	*Komen et al. (1984)*				X
	Janssen (1991)	X	X	X+	
S_{nl4}	*Hasselmann et al. (1985)*	X	X	X	X
S_{nl3}	*Eldeberky (1996)*		NA	NA	NA
S_{ds}	*Komen et al. (1984)*				X
	Janssen (1991)	X	X	X	
S_{bf} Dissipation const. (m^2s^{-3})	*Hasselmann et al. (1973)*	X 0.038	X 0.038	X 0.038	X 0.038
Sbr	*Battjes and Janssen (1978)*	NA	NA	NA	NA
Growth limiter	*Ris (1997)*		X		X
	Hersbach and Janssen (1999)	X		X	
Depth refraction: January Storm Lake Erie		NA X	NA X	NA X	NA X
Propagation scheme		1st order upwind explicit	Fully implicit		
Source term integration scheme		Fully implicit	Fully implicit		

X+ is the corrected SWAN implementation of WAM4
NA = Not Activated

3. The wave model setup and wind input

WAM4.5 and SWAN are used to simulate wave heights for two case studies, namely, the northwest Atlantic storm of 20-22 January 2000 and Lake Erie for the period 12 November – 4 December 2003. For the January storm, simulations are done on two grids shown in Fig. 1, that is, a coarse grid with a resolution of 0.5^o covering the area 25^oN - 70^oN and 82^oW - 0^oW and a fine grid with a resolution of 0.1^o nested within the coarse grid and covering the area 40^oN - 52^oN and 74.5^oW - 46^oW. WAM4.5 runs on the coarse grid while the SWAN model and a nested version of the WAM4.5 run on the fine grid using the boundary conditions provided by the coarse grid WAM4.5. Fig. 2 shows

the computational domain and bathymetry for Lake Erie with the two models running on the same grid with a spatial resolution of 0.05^o. The spectral resolution provides for 25 frequencies logarithmically spaced at intervals of $\delta f/f = 0.1$ from 0.042 Hz to 0.41 Hz for the January storm and from 0.05 Hz to 0.49 Hz for Lake Erie and 24 directional bands at 15^o each with the first direction being 7.5^o measured clockwise from true north. Both models run in shallow water mode in which the bottom friction source term is activated while depth refraction is activated only for the Lake Erie case.

The two models are forced by the 10 m level surface winds obtained from the Canadian Meteorological Centre (CMC) Global Environmental Multiscale (GEM) regional weather prediction model at three-hourly intervals. The wind dataset is created by assembling the 00, 03, 06 and 09 forecast hour winds of the 0000 UTC and 1200 UTC daily runs of the GEM model to produce quasi-hindcast datasets for the January storm (17-23 January 2000) and for Lake Erie (10 November – 4 December 2003) simulation periods, respectively. The winds are first generated on the GEM model grid and then interpolated onto the wave model grids. For the Lake Erie runs the wave models use the same wind inputs. For the January storm runs the same fine grid wind field drives both the nested WAM4.5 and SWAN and ice is not a factor since there are no ice points in the area of interest traversed by the storm. For each run the model is spun up for the first two days of the simulation period to create model initial states, following which the model outputs are then validated against observations.

In this study the WAM4.5 runs are identified as WAM45-CG for the WAM4.5 coarse grid run and WAM45-FG for the WAM4.5 fine grid run, respectively, for the January 2000 storm and as WAM4.5 for the Lake Erie case. The SWAN version 40.72 runs are identified as SWN4072-WAM3 for the run using WAM3 (Komen) physics and SWN4072-WAM4+ for the run using the modified implementation of SWAN WAM4 physics. The third SWAN run based on version 40.31 is identified as SWN4031-WAM4 for the run using WAM4 (Janssen) physics as originally implemented in SWAN to highlight the differences in SWAN results based on the corrected (version 40.72) and uncorrected (version 40.31) implementations of SWAN WAM4. The options used in WAM4.5 and SWAN in this study are described in more detail in Lalbeharry et al. (2009a, 2009b) and are summarized in Table 1.

4. Results and discussion

a. *January 2000 storm case*

The storm of 20-22 January 2000 was a "superbomb" (Perrie et al., 2005) that passed through the middle of the East Coast buoy network with the observed and the CMC GEM model 00H forecast tracks shown in Fig. 3. This storm generated extreme waves of 12 m measured by the waverider RG3 shown in Fig. 1 and produced two exceptionally large waves close to 16 m, and about 10 minutes apart, that hit Port-aux-Basques, Newfoundland (MacPhee, unpublished manuscript). Fig. 4 compares the significant wave heights H_s obtained from the three runs of SWAN at four buoy locations in order to determine their relative performances when compared with each other and against observations. It is seen that the SWN4031-WAM4 run underpredicts the H_s when compared with the H_s from both the SWN4072-WAM3 and SWN4072-WAM4+ runs in all cases. The results of the SWN4072-WAM4+ run based on the inclusion of the shift

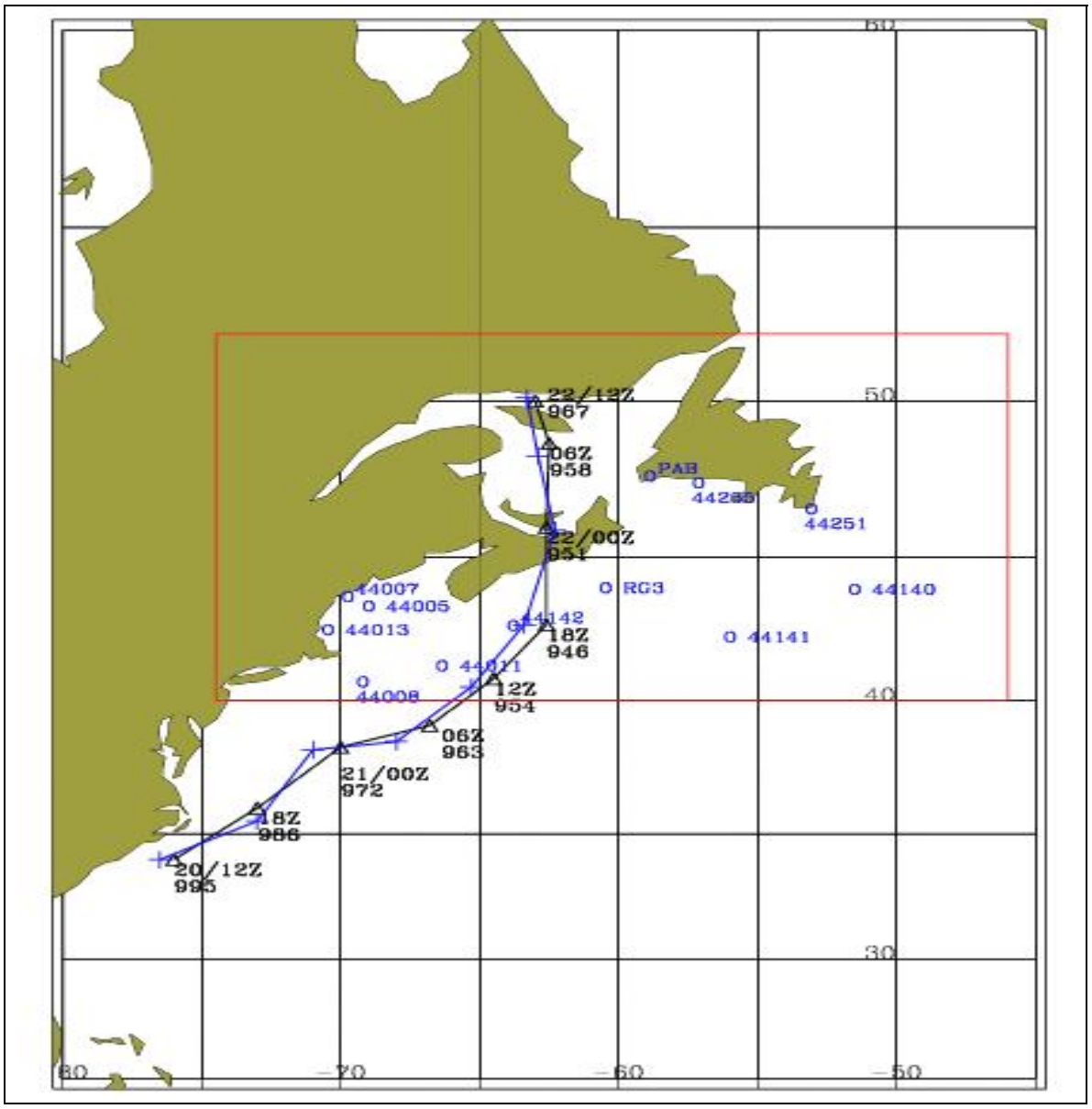

Fig. 3. Storm tracks at 6-hourly intervals for the period 20 -22 January 2000. The observed track is given by the solid black line with the symbol "Δ" with the lower number being the observed central pressure in hPa. The solid blue line with the symbol "+" is the CMC regional GEM model 00H forecast track. The fine grid area is shown by the enclosed box in red lines. Also shown are the locations of the buoys relative to the storm track inside the fine grid used for validation. The buoy identification numbers and locations are the same as given in Fig. 1.

parameter z_α = 0.011 and the wave growth limiter of HJ99 are in good agreement with those of the SWN4072-WAM3 run based on the WAM3 physics of Komen et al. (1984) which is the default option used in SWAN. This suggests that the WAM4 physics as implemented in SWAN version 40.31 is in error. The improved H_s from SWN4072-WAM4+ can, therefore, be ascribed to the inclusion of z_α and the use of the limiter HJ99 in SWAN version 40.72 since other factors such as source terms, numerical schemes, winds and grid resolutions in the two runs are identical. Similar results are also found by

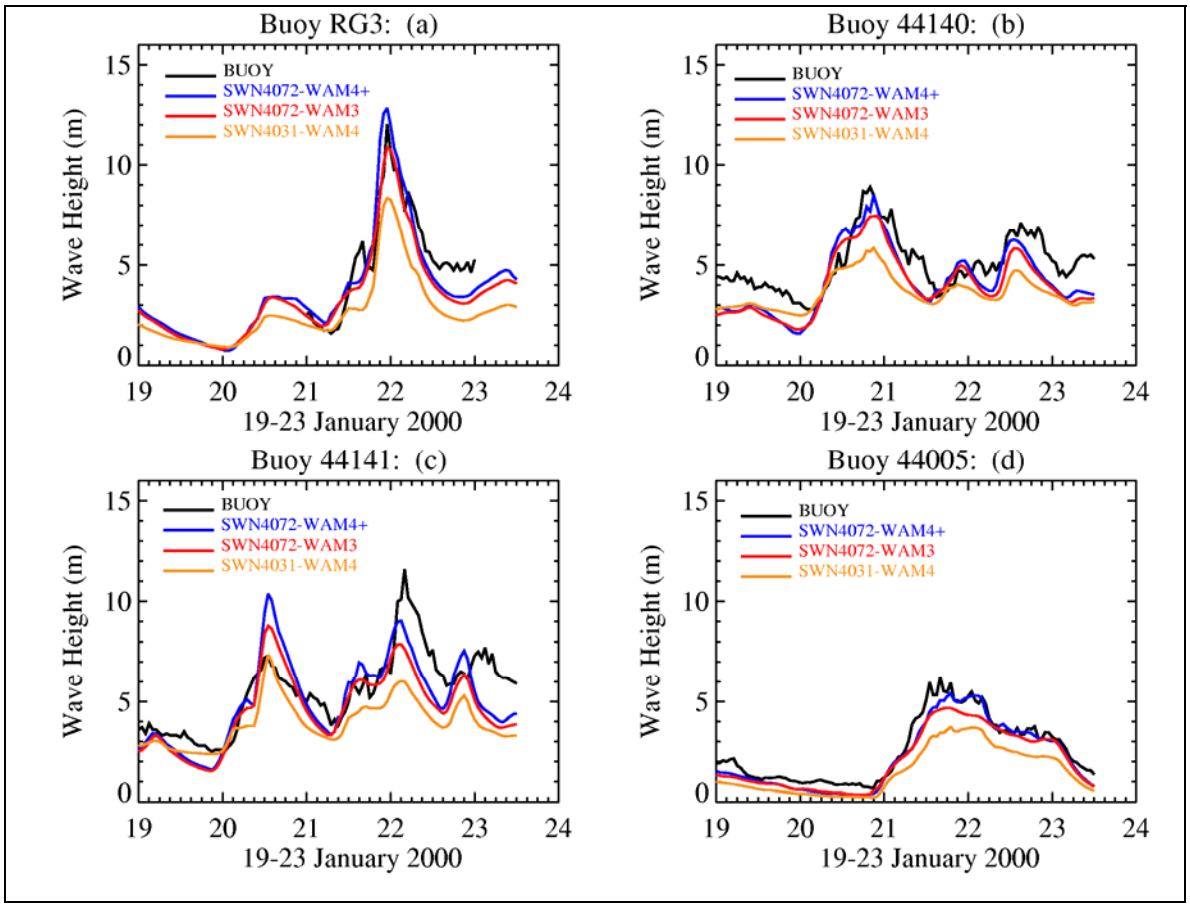

Fig. 4. The significant wave heights, H_s, for the three SWAN runs identified in section 3 are compared against the buoy H_s at 4 locations for the period 19-23 January 2000. The black line gives the buoy H_s, the blue line the SWN4072-WAM+ H_s, the red line the SWN4072-WAM3 H_s and the orange line the SWN4031-WAM4 H_s which is based on the original SWAN implementation of Janssens's WAM4 physics.

Lalbeharry et al (2004). Since it is established that the SWN4072-WAM4+ H_s is an improvement over that based on SWN4031-WAM4, subsequent SWAN results presented are those based on SWN4072-WAM4+ but for completeness and comparison, scatter and time series plots may also be shown for all three SWAN runs.

Fig. 5 displays the significant wave height, H_s obtained from the WAM45-CG, WAM45-FG and SWN4072-WAM4+ runs at six buoy locations. An examination of this figure reveals that the timings of the various H_s peaks of the model runs are well replicated but the intensities of these peaks are replicated in some instances and not so in others. A case in point is the overprediction by all three runs of the observed peak H_s of 8.5 m around 09:00 UTC on 22 January at buoy 44255 in Fig. 5b. This overprediction of 1.5 m to 3.0 m by both WAM4.5 and SWAN is due to the role of model dynamic fetch (Lalbeharry et al., 2009a). Another case is the reported peak H_s of 12 m around 0000 UTC 22 January by the waverider RG3, located just to the right of the storm track, in Fig. 5a. The three model runs produce excellent agreement with the observed peak H_s both in terms of intensity and arrival time. The wave growth and decay phases are well replicated by the three model runs. Differences between the WAM45-CG (blue curves) and

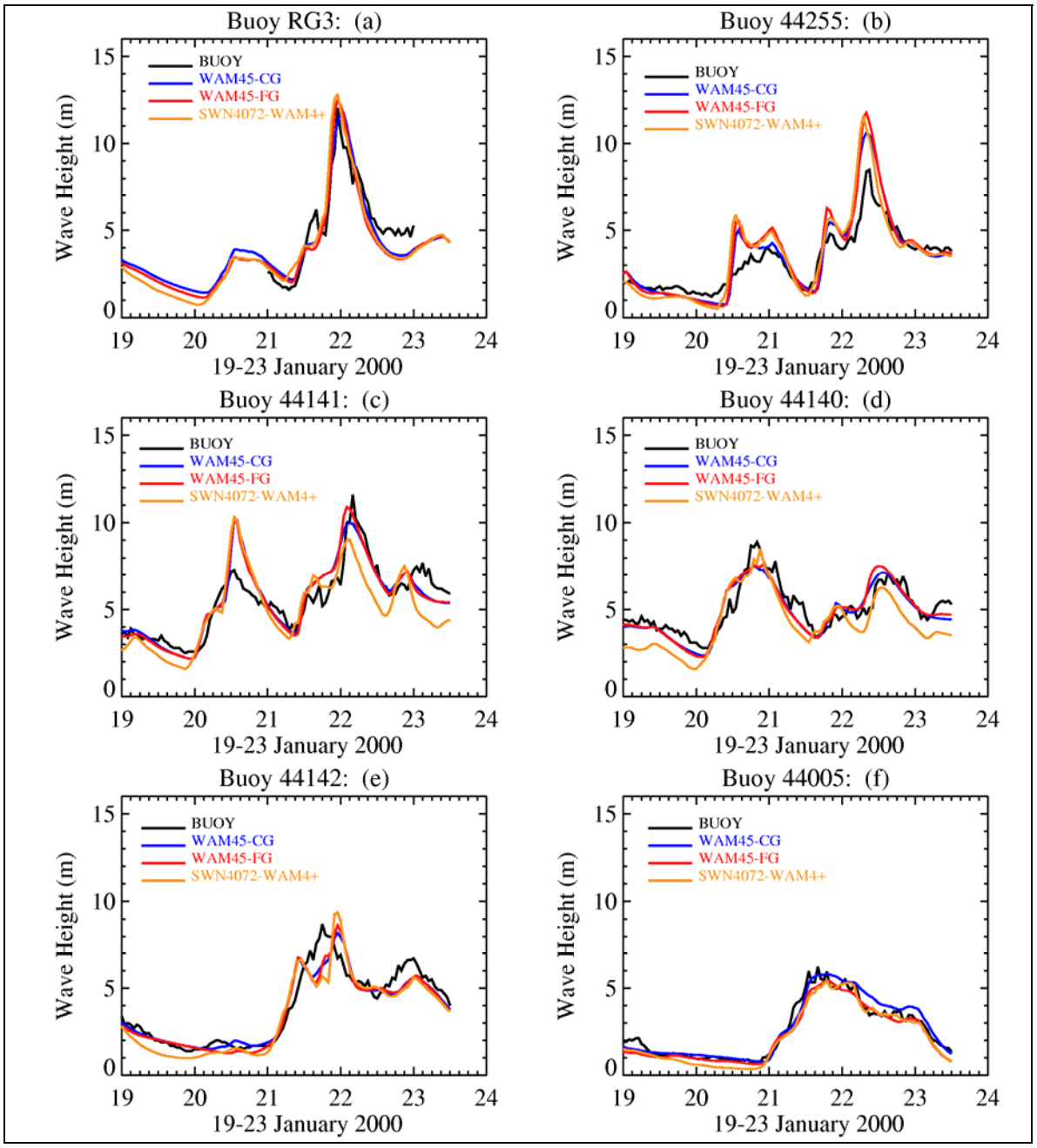

Fig. 5. Time series of observed and model H_s at 6 buoy locations for the period 19-23 January 2000. The black line gives the buoy H_s, the blue line the WAM45-CG H_s, the red line the WAM45-FG H_s and the orange line the SWN4072-WAM4+ H_s which is the corrected version of the original SWAN implementation of Janssen's WAM4 physics.

WAM45-FG (red curves) runs are minimal. This suggests that for open water applications the coarse resolution WAM4.5 is adequate to simulate extreme waves associated with this storm event and that a high resolution WAM4.5 may not be necessary except for nearshore applications given that submerged bathymetric features and small islands are adequately resolved by the coarse grid resolution. Comparison of

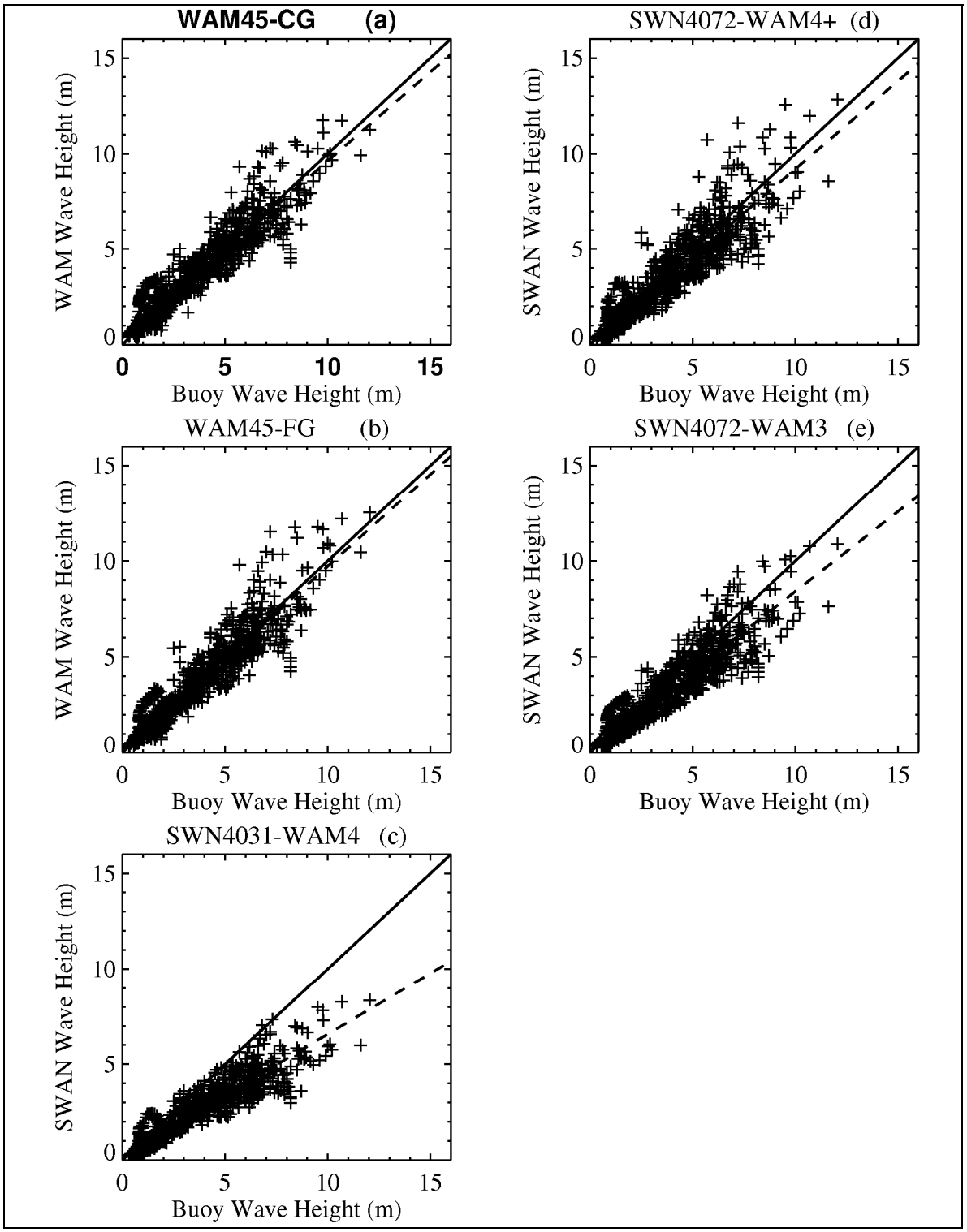

Fig. 6. Scatter plots of model versus observed wave heights for the period 19-23 January 2000. The plot identifications for the 5 model runs are defined in section 3.

the peak H_s of SWN4072-WAM4+ (orange curves) with that of WAM45-FG (red curves) shows reasonably good agreement for some of the peaks. At buoy locations

where the agreement is good, the wave climate is locally windsea dominated and where the agreement is not so good, for example, the second peak in Fig. 5c and in Fig.5d, respectively, and to a lesser extent the major peak in Fig. 5e, the local wave climate is swell dominated (Lalbeharry et al., 2009a). This disagreement may be due to the propagation scheme used by SWAN in nonstationary mode in which the so-called garden-sprinkler effect may show up for propagation over large distances and to the difference in the swell separation methods used by SWAN and WAM4.5.

Scatter plots of model versus buoy wave heights for the period 19-23 January 2000 are presented in Fig. 6. Only the buoys inside the fine grid shown in Fig. 1 are used to produce the plots. The solid black lines denote perfect fit to model and observed values and the dashed lines the best fit linear regression lines. The plots provide a more appealing way of displaying the same statistical information. Wave heights in excess of about 5 m are better predicted by both the WAM45-CG and WAM45-FG shown in Fig. 6a and Fig. 6b, respectively, while the SWN4072-WAM+ and SWN4072-WAM3 give somewhat more spread as confirmed by the regression lines in Fig. 6d and Fig. 6e, respectively. The SWN4031-WAM4 in Fig. 6c consistently underpredicts the wave heights. For a given buoy wave height, the regression lines for the two WAM4.5 runs give a better estimate of the corresponding model wave height than the regression lines for the three SWAN runs. It is obvious also that the SWN4031-WAM4 regression line gives a much lower estimate of the model wave height than the SWN4072-WAM4+ regression line.

b. Lake Erie case

WAM4.5 and SWAN are applied over Lake Erie in a hindcast mode for a three-week period 12 November – 4 December 2003. The period is chosen because it includes a remarkable storm event which generated high wind speeds and significant wave heights at 1500 UTC on 13 November in the north-eastern part of the lake. In this case SWAN is not nested inside the WAM4.5 as was done in the January 2000 storm case. The two models run on the same grid with a spatial resolution of 0.05° in both latitude and longitude directions and use same wind input. The maximum dimensions of Lake Erie are about 400 km in length and 100 km breadthwise and the water depths ranges from 5 – 60 m as shown in Fig. 2. This lake can, therefore, be considered shallow enough to be used as a candidate for testing the models in shallow or transitional water depth mode as defined in WMO (1998) since a significant area of the lake lies in water depths < 25 m. The results obtained by WAM4.5 and SWAN in shallow water mode with depth refraction and without tidal influences are compared with observations at the three buoy locations shown in Fig. 2.

Fig. 7 presents time histories of measured and computed significant wave height (H_s) and peak period (T_p) at buoy location 45132 in water depth of 22 m, Fig. 8 those at buoy location 45142 in water depth of 27 m and Fig. 9 those at buoy location 45005 in water depth of 14 m. The wave observations for buoy 45142 are valid up to 0000 UTC 22 November, after which the observations are not valid because of instrument malfunction or the buoy ceases to make observations. The main purpose of these figures is to show how well the WAM4.5 performs when compared with the coastal model SWAN at intermediate water depths such as Lake Erie. It is seen from these figures that the various

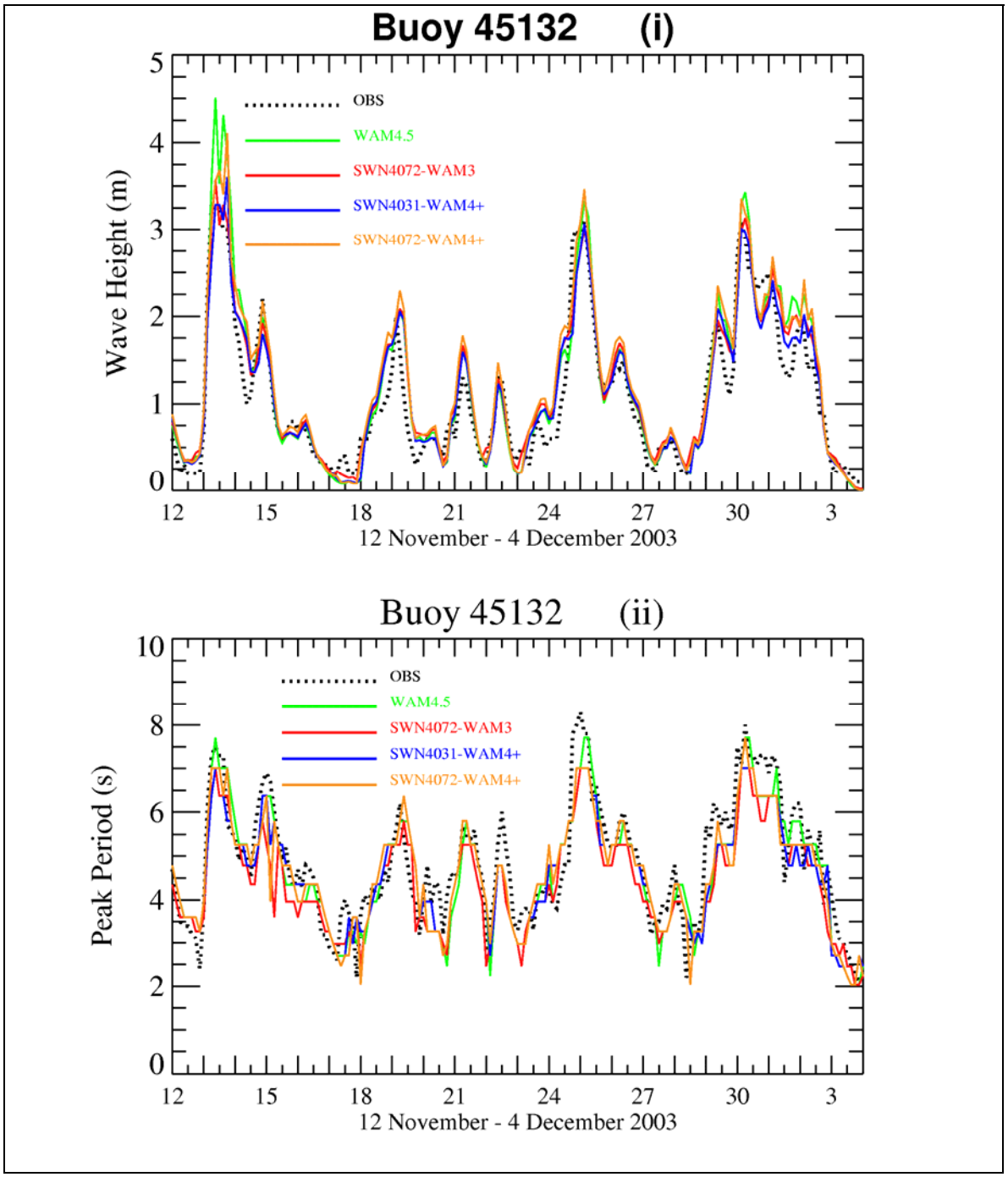

Fig. 7. Time series of observed and model (i) significant wave heights and (ii) peak wave periods at buoy location 45132 for the time period 12 November - 4 December 2003. The figure legends are defined in section 3.

H_s peaks, the corresponding T_p and their arrival times are well replicated by both WAM4.5 and the three SWAN runs.

In Fig. 7(i) at the buoy 45132 three main wave episodes can be detected on 13, 25 and 30 November, with the most pronounced one at 1500 UTC 13 November. These

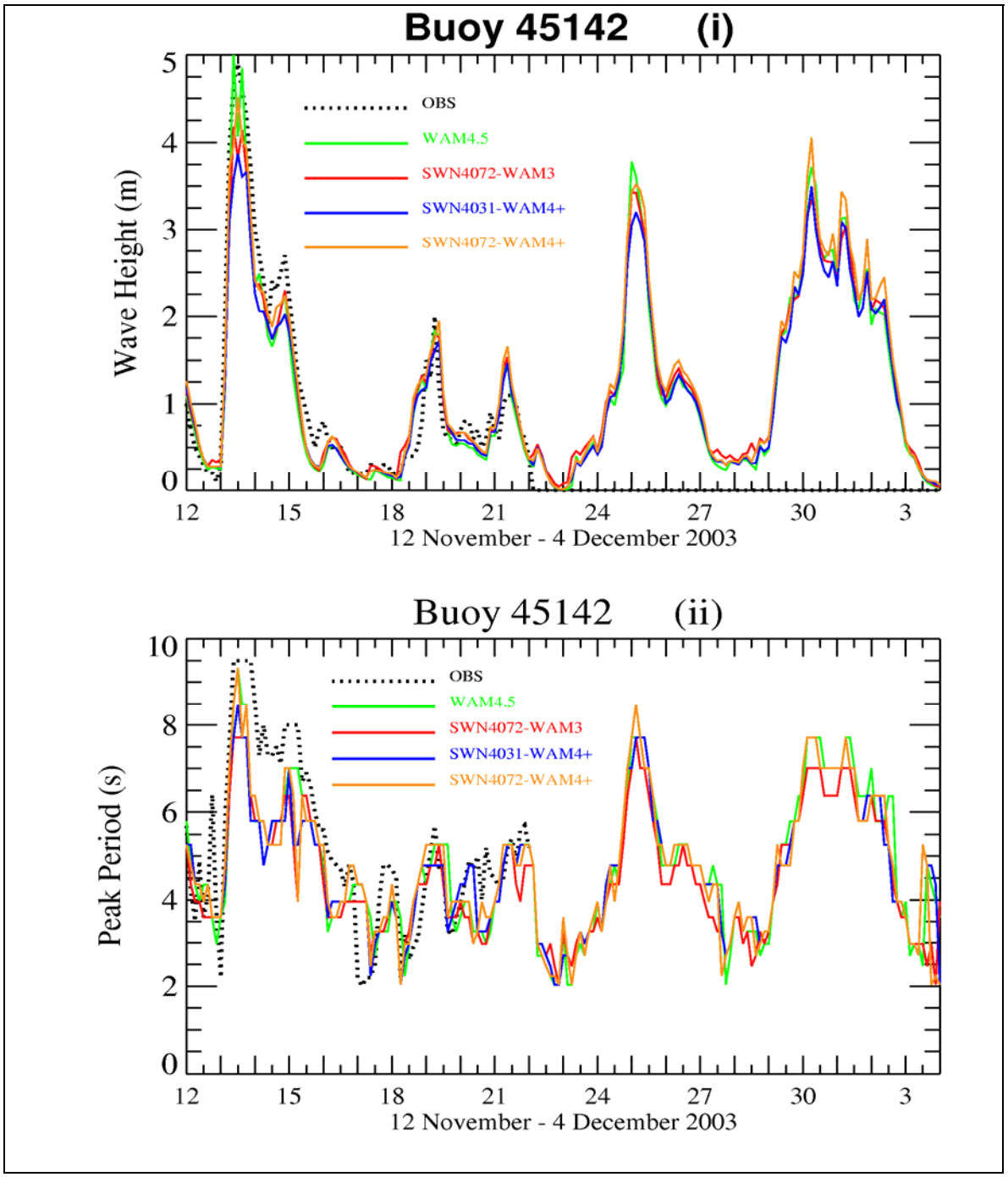

Fig. 8. Same as Fig. 7 but at buoy location 45142.

events are associated with T_p of 8 s or less as shown in Fig. 7(ii), suggesting that the local wave climate is predominantly windsea. The agreement between the measurements and the results of the two wave models is very good for the significant wave heights. The measured peak H_s values in the three abovementioned episodes are only slightly overestimated by the wave models with the biggest difference of about 1.2 m occurring at the first and highest peak at 1500 UTC 13 November between the buoy and WAM4.5

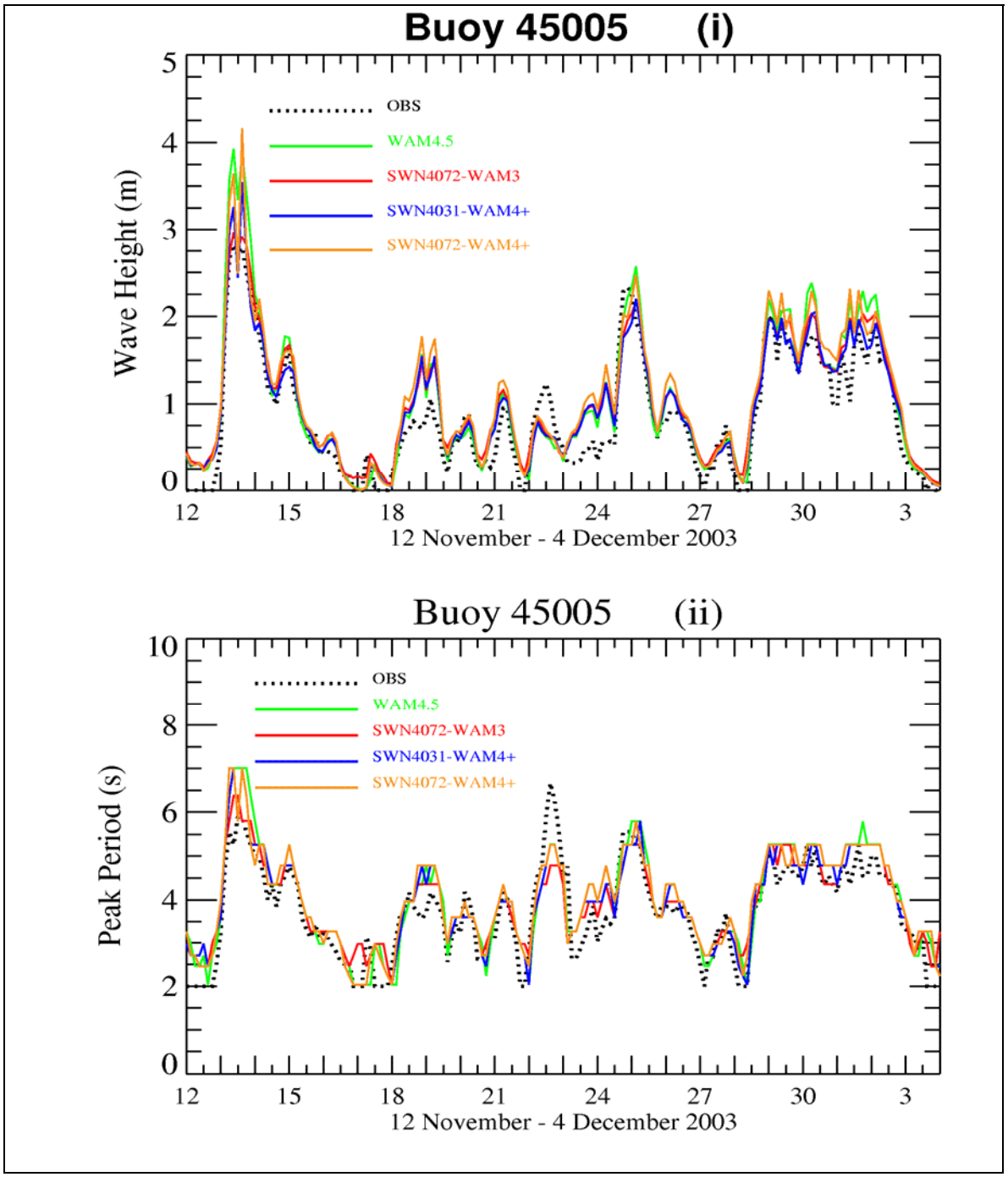

Fig. 9. Same as Fig. 7 but at buoy location 45005.

values. This overprediction of the wave height is also reflected in the overprediction of the wind speed (Lalbeharry et al., 2009b) at that time. The results of SWAN are closer to the observed value for this special peak than WAM4.5. In contrast to the wave height comparisons, Fig. 7(ii) indicates WAM4.5 performs better than SWAN for the peak periods. The model results shown in Fig. 8 at buoy 45142 located in the northeast corner of the lake (see Fig. 2) are quite similar to those obtained at buoy 45132 during the period

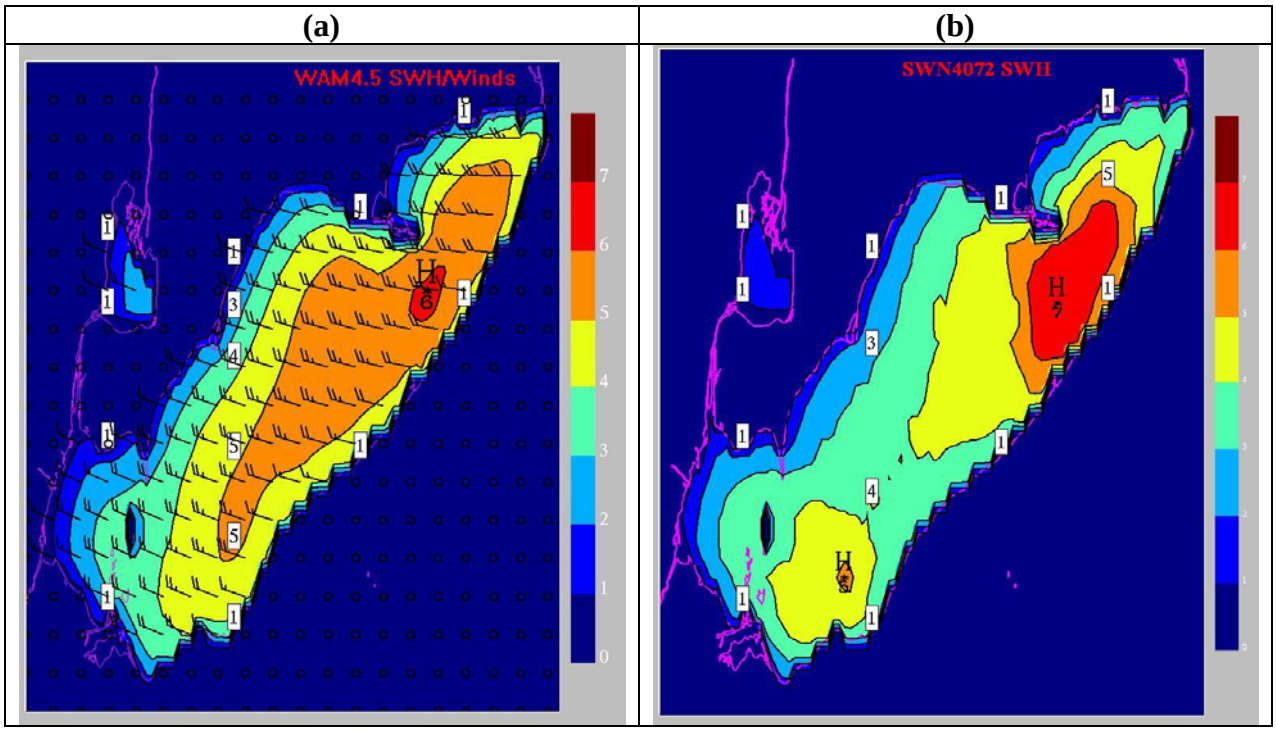

Fig. 10 Snapshots of (a) WAM4.5 H_s and (b) SWN4072-WAM4+ $_{Hs}$ valid 1500 UTC 13 November 2003. The corresponding wind field input to the two models is superimposed on (a). The H_s contours are given in metres and the winds in meteorological convention with full barb as 10 ms^{-1} and half-barb as 5 ms^{-1}. In the figure H indicates the maximum central value.

of observations at buoy 45142. It is interesting to note that the WAM4.5 peak H_s of 5 m agrees exactly with the observed value while the three SWAN runs slightly underpredict this peak. However, SWN4072-WAM4+ is in better agreement with the buoy measurement than both SWAN4031-WAM4+ and SWAN4072-WAM3. The WAM 4.5 T_p close to 9 s agrees reasonably well with the observed T_p of 10 s. Fig. 9 displays the same time series plots as in Fig. 7 but at buoy 45005. The major wave episode also occurs here at 1500 UTC 13 November with the observed peak H_s being 3 m. In this case WAM4.5 overestimates this peak by about 1.0 m in response to the slight overprediction of the wind speed (Lalbeharry et al., 2009b). However, SWN4072-WAM3 peak $H_{s,}$ is in better agreement with the observed peak than the corresponding peaks of the other two SWAN runs.

Snapshots in Fig. 10 show the spatial distributions of (a) WAM4.5 H_s and (b) SWN4072-WAM4+ H_s valid 1500 UTC 13 November 2003. The corresponding wind field common to the two models is superimposed on the H_s field in Fig. 10a. At that time north-westerly winds are prevailing with wind speeds reaching about 25 ms^{-1} and model-generated H_s reaching 6 m or more in the northeastern part of the lake. The model wave conditions generated at the three buoy locations shown in Figs. 10a and 10b are also remarkable, especially taking into account that wind fetch and duration for the development of the waves at these locations are relatively short. The two models generate peak H_s up to 6 m or more mainly in the same location although the area enclosed by the

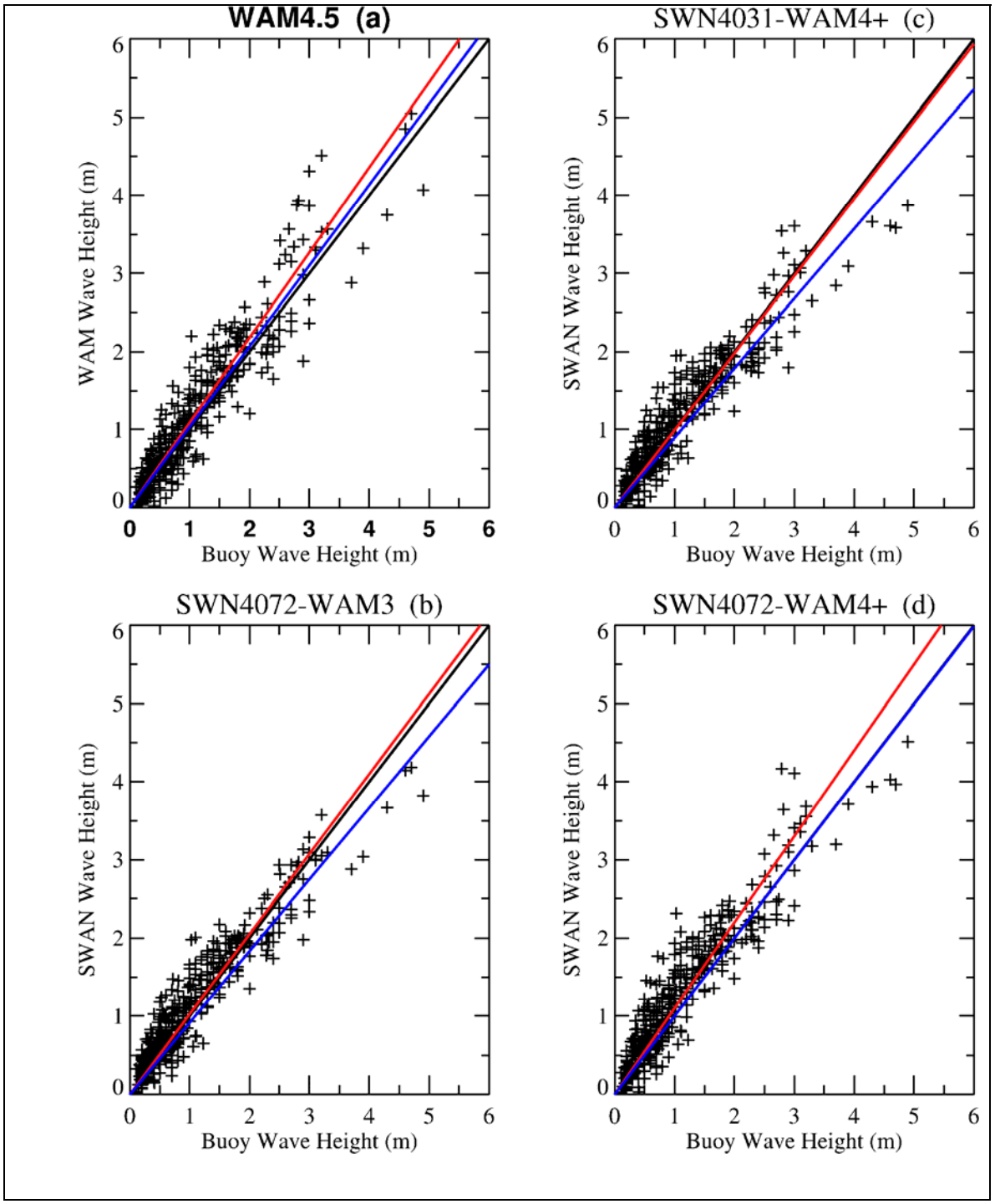

Fig. 11. Scatter plots of model versus observed wave heights based on observations at buoys 45005, 45132 and 45142 for the time period 12 November – 4 December 2003. The black lines denote the perfect fit to model and observed values, red lines the lines with symmetric slope, s and blue lines the best fit linear regression lines. Model values are overpredicted for s > 1.0 and underpredicted for s < 1.0. The plot identications are define in section 3.

6 m contour varies from one model to the other. It should be noted that buoy 45142 in vicinity of the 6 m contour recorded a peak H_s of 5 m and lends credence to the model generated wave heights of 6 m or more.

Fig. 11 presents scatter plots of model versus buoy significant wave heights >= 0.1 m for the period 12 November – 4 December 2003. The plots are based on the available observations at buoys 45132, 45005 and 45142. The plots indicate that a maximum value close to 5 m is observed by the buoy and simulated by WAM4.5 while SWAN generated a value between 4 – 4.5 m. The observed value near 5 m appears in the time series plots of the wave heights in Fig. 8(i) at buoy location 45142. The symmetric slope (red line) is close to 1.0 (SWN4031-WAM4+) or slightly > 1.0. This is the regression coefficient of the line constrained to pass through the origin obtained by fitting data pairs of model and observed values (Bauer et al., 1992). It gives a measure of the deviation of the data pairs from the perfect fit straight line. Hence, WAM4.5 and the most recent version SWN4072-WAM4+ show a small tendency to overestimate H_s. The scatter plots appear quite similar in features indicating minimal differences between the two models.

5. Conclusions

Two state-of-the-art third generation ocean wave models, namely, the WAM4.5 and SWAN, are utilized in numerical wave simulations of the extreme storm of 19-23 January 2000 over the Northwest Atlantic and in the generation of waves over Lake Erie for the period 12 November – 4 December 2003. The latter period is chosen because it includes a remarkable storm event which generated high wind speeds and significant wave heights at 1500 UTC on 13 November in the north-eastern part of the lake. In the original implementation of the SWAN version of WAM4, the shift growth parameter was omitted in the wind input source term, the omission of which apparently led to underprediction of the significant wave heights. Inclusion of this parameter and the Hersbach-Janssen wave growth limiter as an option when the WAM4 option is chosen in SWAN causes a slight enhancement of the normalized growth rate and results in better agreement with the observed wave heights. The three runs of SWAN include the run using the Komen WAM3 physics (the default option in SWAN), that using Janssen WAM4 physics as originally implemented in SWAN and that using the modified implementation of SWAN WAM4 physics. SWAN version 40.31 was originally applied to both cases (Lalbeharry et al., 2009a, 2009b) but in this study the two cases are revisited using the most recent SWAN 40.72 version as well as some results from version 40.31.

For the January 2000 storm case the results presented are for a specific storm case and, therefore, may not be generalized to larger samples, or even other storms. WAM4.5 runs on a coarse grid while SWAN and a nested version of WAM4.5 run on a fine grid using the boundary conditions provided by the coarse grid WAM4.5. The modified version of the SWAN implementation of WAM4 produces wave results that are more accurate than those of the unmodified version and are in closer agreement with those using the SWAN WAM3 option and WAM45-FG. The improved significant wave height from both SWN4072-WAM4+ and SWN4031-WAM4+ runs is ascribed to the modifications made to the original implementation of SWAN WAM4 since other factors such as source terms, numerical schemes, winds and grid resolutions in the two SWAN

runs are identical. Differences between the WAM45-CG and WAM45-FG runs are minimal. This suggests that for open and intermediate water depths the coarse grid WAM4.5 with a grid resolution of 0.5^{o} can be used in operational applications to simulate extreme waves associated with this storm event and that a high resolution WAM4.5 may not be necessary except for nearshore applications given that submerged bathymetric features and small islands are adequately resolved by the coarse grid resolution. The agreement between the peak H_s of the SWN4072-WAM4+ run and that of the WAM45-FG is reasonably good at buoy locations where the sea is locally windsea dominated and not so good where the sea state is swell dominated.

For Lake Erie both WAM4.5 and SWAN run on the same grid using the same wind input. In this case SWAN is not nested inside the WAM4.5 as was done in the January 2000 storm case. The performances of the two models indicate that WAM4.5 seems to be a reasonable choice for use in an operational environment instead of the coastal wave model SWAN in an application on such intermediate scale in an enclosed water basin such as Lake Erie.

Acknowledgements
The authors wish to express their sincere thanks to SEIMAC Limited, Dartmouth, NS and COA Coastal Ocean Associates INC. for providing waverider data from oil and gas platforms operating near Sable Island. Other archived wave data were provided by the Marine Environmental Data Service, Fisheries and Oceans, Canada, and the NOAA National Data Buoy Centre.

References

Battjes, J. A. and J. P. F. M. Janssen, 1978. Energy loss and set-up due to breaking of random waves. Proc. Coastal Eng. Conf., 16th, 569-587.

Bauer, Eva, Susanne Hasselmann and Klaus Hasselmann, 1992. Validation and assimilation of Seasat altimeter wave heights using the WAM wave model. J. Geophys. Res., 98C, 12671-12692.

Booij, N., R. C. Ris and L. H. Holthuijsen, 1999. A third generation wave model for coastal regions 1. Model description and validation. J. Geophy. Res., 104, C4, 7649-7666.

Cavaleri, L. and P. Malanotte-Rizzoli, 1981. Wind wave prediction in shallow water: Theory and applications. J. Geophys. Res., 86, 10961-10973.

Eldeberky, Y. 1996. Nonlinear transformation of wave spectra in the nearshore zone. Ph.D. thesis, Delft University of Technology, Department of Civil Engineering, The Netherlands.

Hasselmann, K., T. P. Barnett, K. Bouws, H. Carlson, D. E. Cartwright, K. Enke, J. I. Ewing, H. Gienapp, D. E. Hasselmann, P. Kruseman, A. Meerburg, P. Muller, K. Richter, D. J. Olbers, W. Sell and H. Walden (1973). Measurements of wind-wave growth and swell decay during the Joint North Sea Wave Project (JONSWAP), Dtsch. Hydrogr. Z. Suppl., 12, A8, 95p.

Hasselmann, K., D. B. Ross, P. Müller, W. Sell, 1976. A parametrical wave prediction model, J. Phys. Oceanogr., 6, 201-228.

Hasselmann, S., K. Hasselmann, J. H. Allender and T. P. Barnett,1985. Computations and parameterizations of the nonlinear energy transfer in a gravity-wave spectrum. Part II: Parameterizations of the nonlinear transfer for application in wave models. J. Phys. Oceanogr., 19, 745-754.

Hersbach, H. and P. A .E. M. Janssen, 1999. Improvement of the short-term behaviour in the wave ocean model (WAM). J. Atmos. Oceanic Techn., 16, 884-892.

Holthuijsen, Leo H., 2007: Waves in Oceanic and Coastal Waters. Cambridge University Press, Cambridge, 387p.

Janssen, P. A. E. M., 1989. Wave-induced stress and the drag of air flow over sea waves J. Phys. Oceanogr., 19, 745-754.

Janssen, P. A. E. M., 1991. Quasi-linear theory of wind-wave generation applied to wave forecasting. J. Phys. Oceanogr., 21, 1631-1642.

Komen, G. J., L. Cavaleri, M. Donelan, K. Hasselmann, S. Hasselmann, and P. A .E. M. Janssen, 1994. Dynamics and Modelling of Ocean Waves, Cambridge University Press, Cambridge, 532p.

Komen, G. J., S. Hasselmann and K. Hasselmann, 1984. On the existence of a fully developed windsea spectrum. J. Phys. Oceanogr., 14, 1271-1285.

Lalbeharry, Roop, Ralph Bigio, Bridget Thomas and Laurence Wilson, 2009a: Numerical simulation of extreme waves during the storm of 20-22 January 2000 using CMC weather prediction model generated winds. ATMOSPHERE-OCEAN 47 (1) 2009, 99-122 doi:10.3137/OC292.2009

Lalbeharry, Roop, Arno Behrens, Heinz Guenther and Laurence Wilson, 2009b: Matching of coastal and open ocean wave models in a mesoscale application over Lake Erie. ATMOSPHERE-OCEAN 47 (3) 2009, 0–00 doi:10.3137/OC305.2009.

Lalbeharry, Roop, Arno Behrens, Heinz Guenther and Laurie Wilson, 2004: An evaluation of wave model performances with linear and nonlinear dissipation source terms in Lake Erie. In: Proc. *8th Int. Workshop on Wave Hindcasting and Forecasting*, North Shore, Oahu, Hawaii, November 14-19, 2004. Available on CD from Environment Canada

Liu, Paul C., David J. Schwab and Robert E. Jensen, 2002. Has wind-wave modeling reached its limit? Ocean Eng., 29, 81-98.

Monbaliu, Jaak, Roberto Padilla-Hernandez, Julia C. Hargreaves, Juan Carlos Albiach, Weimin Luo, Mauro Sclavo and Heinz Guenther, 2000. The spectral wave model, WAM, adapted for applications with high resolution. Coastal Eng., 41, 41-62

Perrie, W., E. L. Andreas, W. Zhang, W. Li, J. Gyakum, and R. McTaggart-Cowan, 2005: Sea spray impacts on intensifying midlatitude cyclones. *J. Atm. Sc*., **62**, 1867-1883.

Ris, R. C., L. H. Holthuijsen and N. Booij, 1999. A third generation wave model for coastal regions 2. Verification. J. Geophy. Res., 104, C4, 7667-7681.

Ris, R. C., 1997. Spectral modelling of wind waves in coastal areas. PhD Thesis, Delft University of Technology, Delft, Netherlands.

Soomere, Tarmo, 2005. Wind wave statistics in Tallinn Bay: Boreal Environmental Research, 10, 103-118.

SWAN (2009) User Manual SWAN Cycle III version 40.72. Delft University of Technology, Department of Civil Engineering, the Netherlands.

SWAN (2004) User Manual SWAN Cycle III version 40.31, February 5, 2004. Delft University of Technology, Department of Civil Engineering, the Netherlands.

Tolman, H. J., 1992. Effects of numerics on the physics in a third generation wind-wave model. J. Phys. Oceanogr., 22, 1095-1111.

WAMDI Group, 1988. The WAM model - A third generation ocean wave prediction model. J. Phys. Oceanogr., 18, 1775-1810.

World Meteorological Organization, 1998. Guide to Wave Analysis and Forecasting, WMO-No. 702, 2nd ed., 159 pp.